

High Photovoltaic Performance of As-casting Device Based on New Quinoxaline-based Donor-Acceptor Copolymers

Mingzhi Zhao,^{1,2} Zi Qiao,^{1,2} Xiaofeng Chen,^{1,2} Chenglin Jiang,^{1,2} Xiaoyu Li,^{2*}

Yongfang Li,³ and Haiqiao Wang^{1,2*}

1. State Key Laboratory of Organic-Inorganic Composite, Beijing University of Chemical Technology, Beijing 100029, China

2. Key Laboratory of Carbon Fiber and Functional Polymers, Ministry of Education, Beijing University of Chemical Technology, Beijing 100029, China

3. Beijing National Laboratory for Molecular Sciences, Institute of Chemistry, Chinese Academy of Sciences, Beijing 100190, China

* Corresponding author: e-mail: wanghaiqiao@mail.buct.edu.cn (H. Wang);

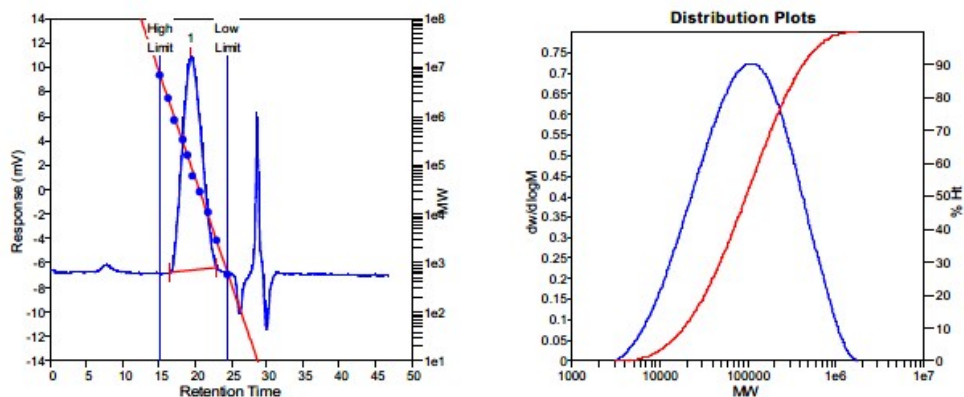
lixxy@mail.buct.edu.cn (X. Li)

Content

1. GPC plot	Figure S1
2. TGA plots of the polymers	Figure S2
3. Thin film cyclic voltammograms of polymers	Figure S3
4. Energy level diagrams	Figure S4
5. Current density–voltage characteristics of the PSCs	Figure S5
6. $J^{1/2} \sim V_{\text{eff}}$ characteristics	Figure S6

7. AFM topography	Figure S7
8. Photovoltaic performances	Table S1
9. ^1H -NMR and ^{13}C -NMR spectra	Figure S8-S16

(a)



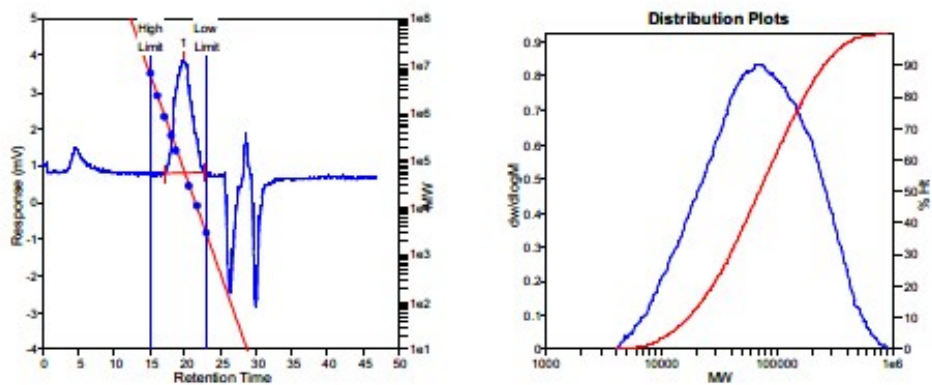
MW Averages

Peak No	Mp	Mn	Mw	Mz	Mz+1	Mv	PD
1	108129	45919	169254	410043	654387	140562	3.68593

Processed Peaks

Peak No	Name	Start RT (mins)	Max RT (mins)	End RT (mins)	Pk Height (mV)	% Height	Area (mV.secs)	% Area
1		16.58	19.38	22.93	17.4603	100	3343.07	100

(b)



MW Averages

Peak No	Mp	Mn	Mw	Mz	Mz+1	Mv	PD
1	70281	40304	108837	223197	341242	94161	2.7004

Processed Peaks

Peak No	Name	Start RT (mins)	Max RT (mins)	End RT (mins)	Pk Height (mV)	% Height	Area (mV.secs)	% Area
1		17.17	19.78	22.68	3.09041	100	518.688	100

Figure S1 GPC plot of polymers: (a) PBDT-DFQX-TTSEH (b) PBDT-DFQX-TTSC8

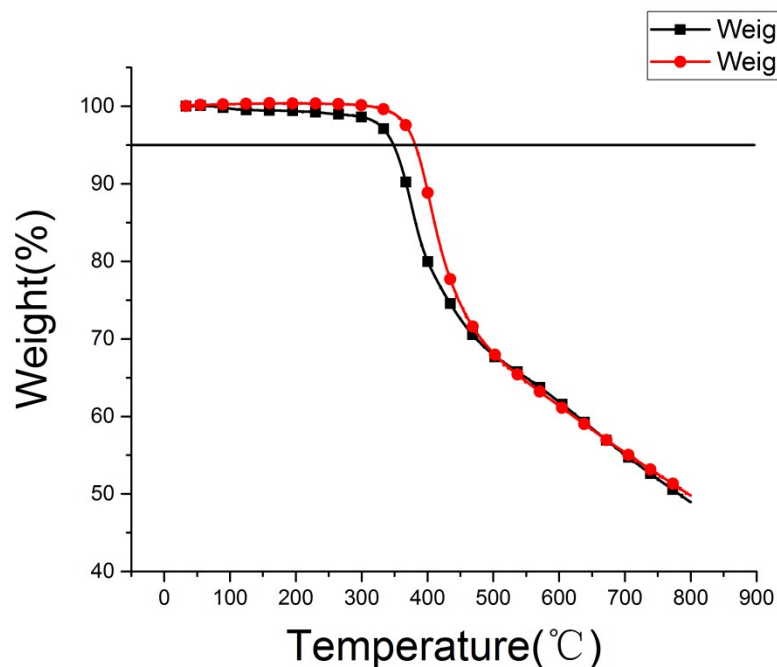


Figure S2 TGA plots of the polymers with a heating rate of 10 C min⁻¹ under a N₂ atmosphere.

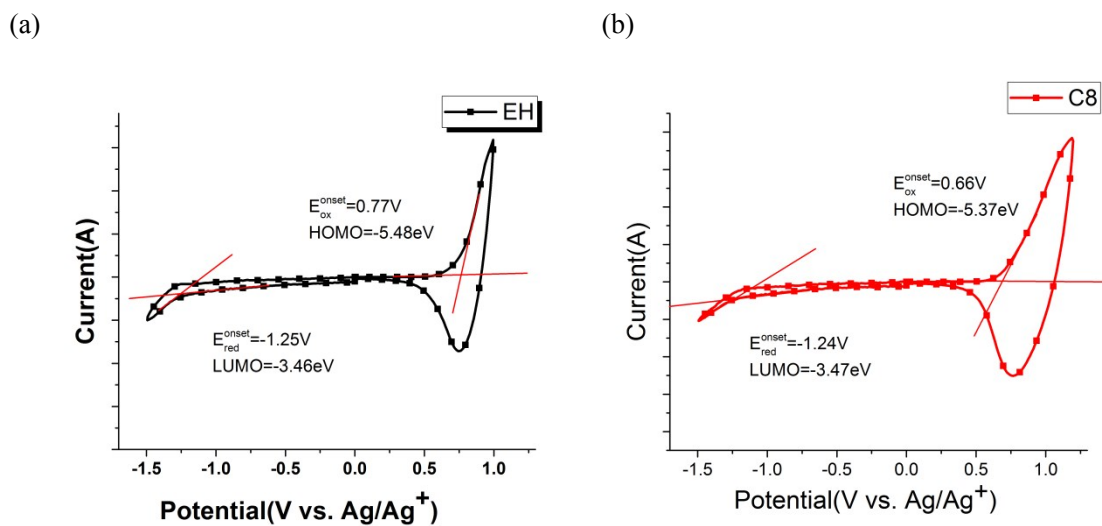


Figure S3 Thin film cyclic voltammograms of PBDTTS-EH-Qx and PBDTTS-C8-Qx in 0.1 M Bu₄NPF₆ acetonitrile solution at a scan rate of 100 mV·s⁻¹

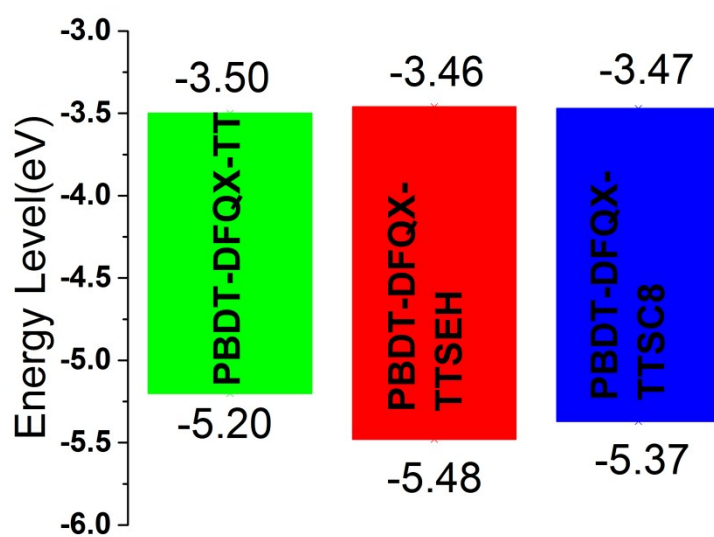


Figure S4 Energy level diagrams for PBDT-DFQX-TT, PBDT-DFQX-TTSEH and PBDT-DFQX-TTSC8

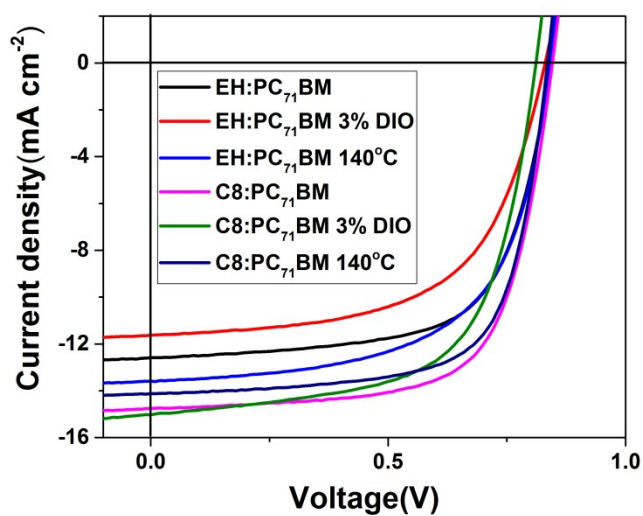


Figure S5 Current density–voltage characteristics of the PSCs based on polymer:PC₇₁BM blends with different treatment under illumination of AM1.5, 100 mW cm⁻²

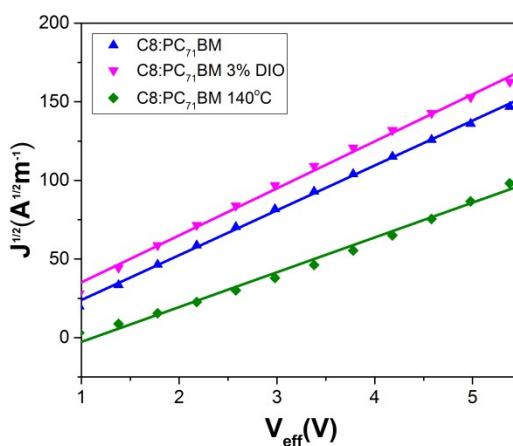
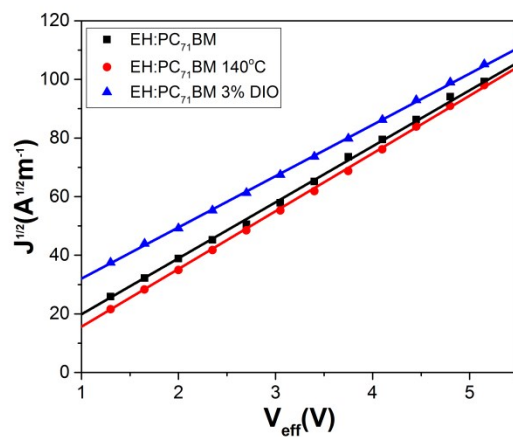


Figure S6 $J^{1/2} \sim V_{\text{eff}}$ characteristics for the devices based on the blend films. Solid lines were the fitting lines of the data.

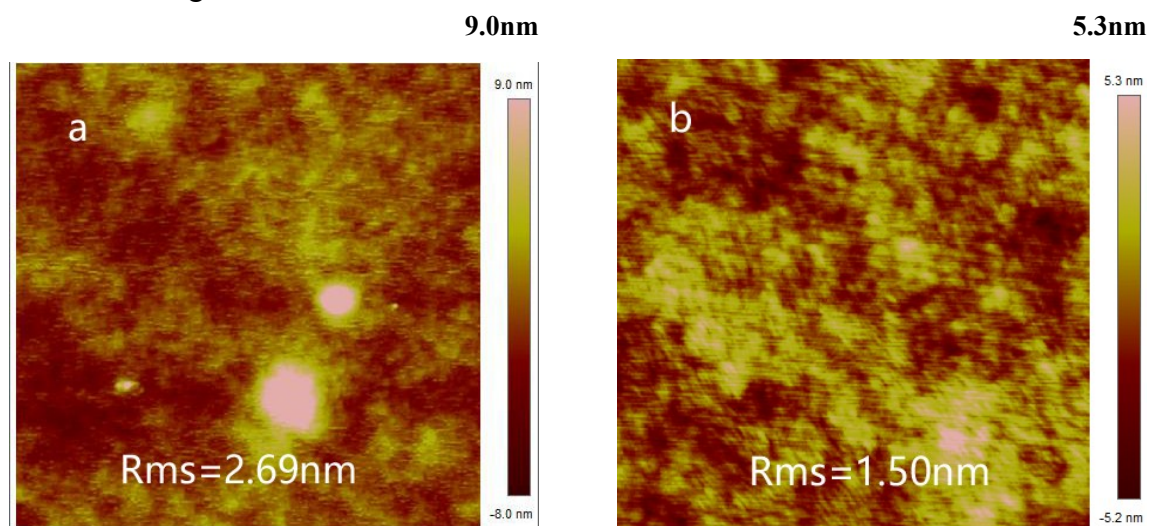


Figure S7 AFM topography ($2.5 \times 2.5 \mu\text{m}^2$) of blend films treat both with DIO and thermal annealing. (a) for PBBDT-DFQX-TTSEH (b) for PBBDT-DFQX-TTSC8

Table S1 Photovoltaic performances of the PSCs based on polymer/PC₇₁BM

under the illumination of AM1.5G, 100 mW·cm⁻².

Polymer	Ratio _a	Treatment	V_{oc} (V)	J_{sc}		
				($mA \cdot cm^{-2}$)	FF(%)	PCE ^b (%)
EH	1:1.2	3%DIO,TA	0.83	12.05	59.11	5.94(5.47 ± 0.36)
C8	1:1.2	3%DIO,TA	0.81	14.04	61.54	6.9(6.80 ± 0.17)

^a Polymer/PC₇₁BM weight ratio. ^b Optimized data. Average data were in the parentheses and obtained from 10 devices.

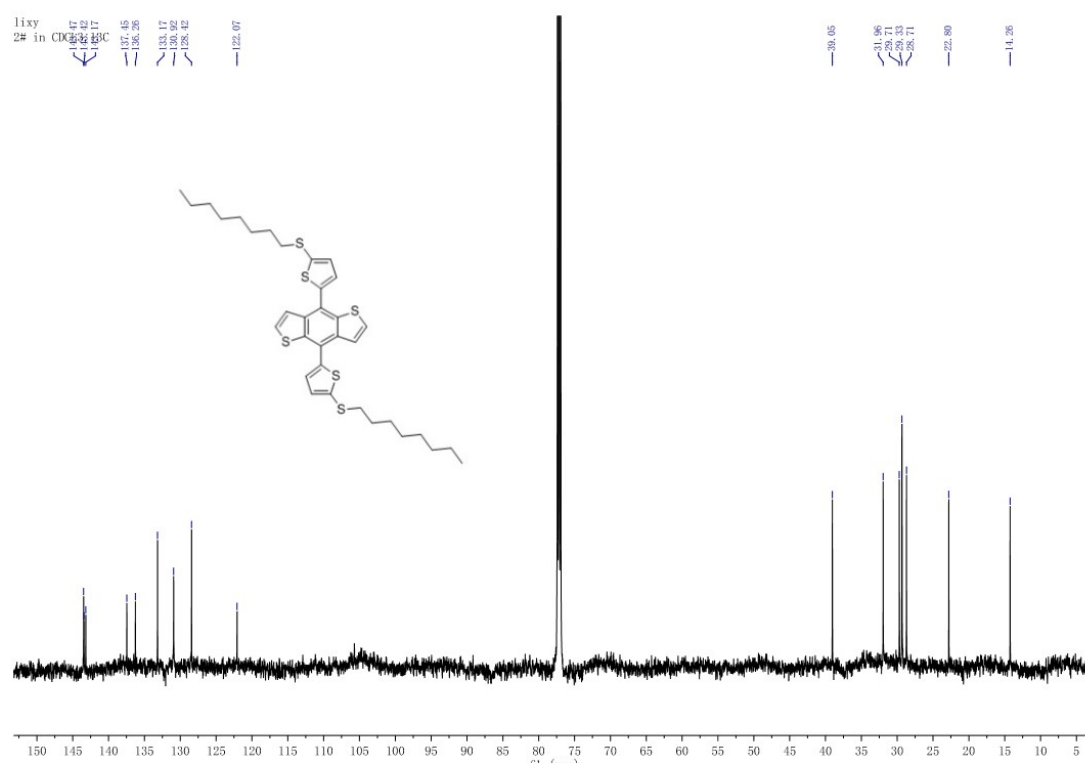


Figure S8 13C-NMR of BDT-TSC8

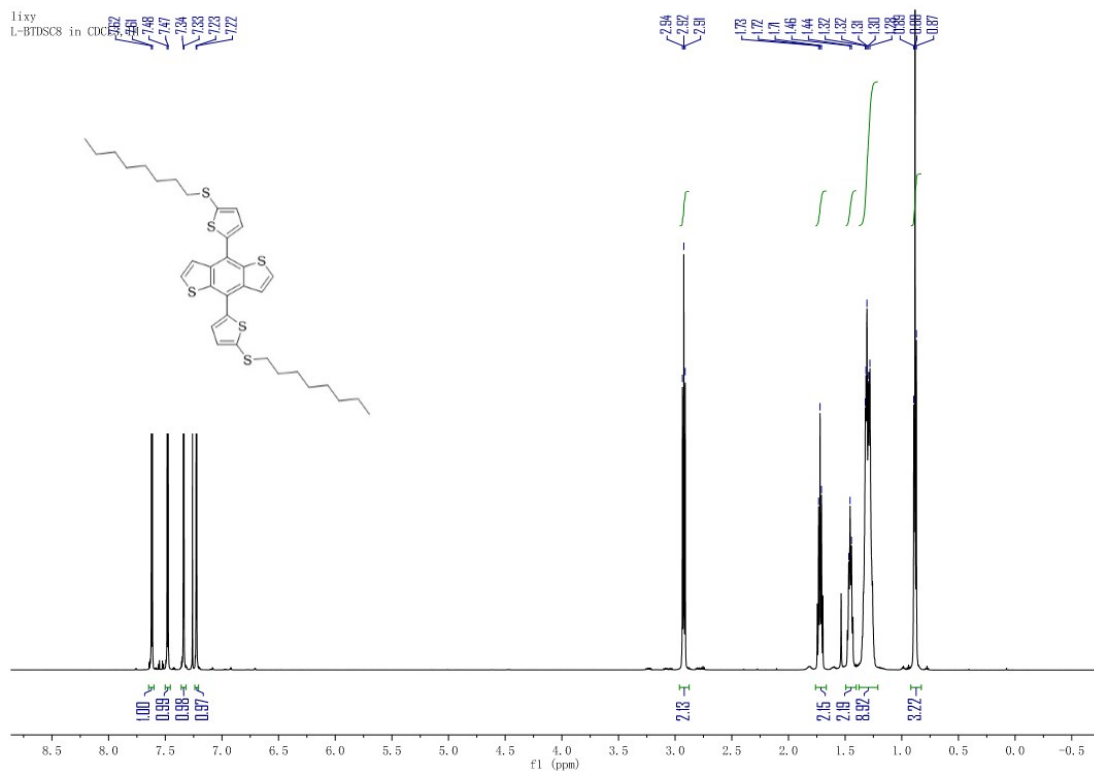


Figure S9 ¹H-NMR of BDT-TSC8

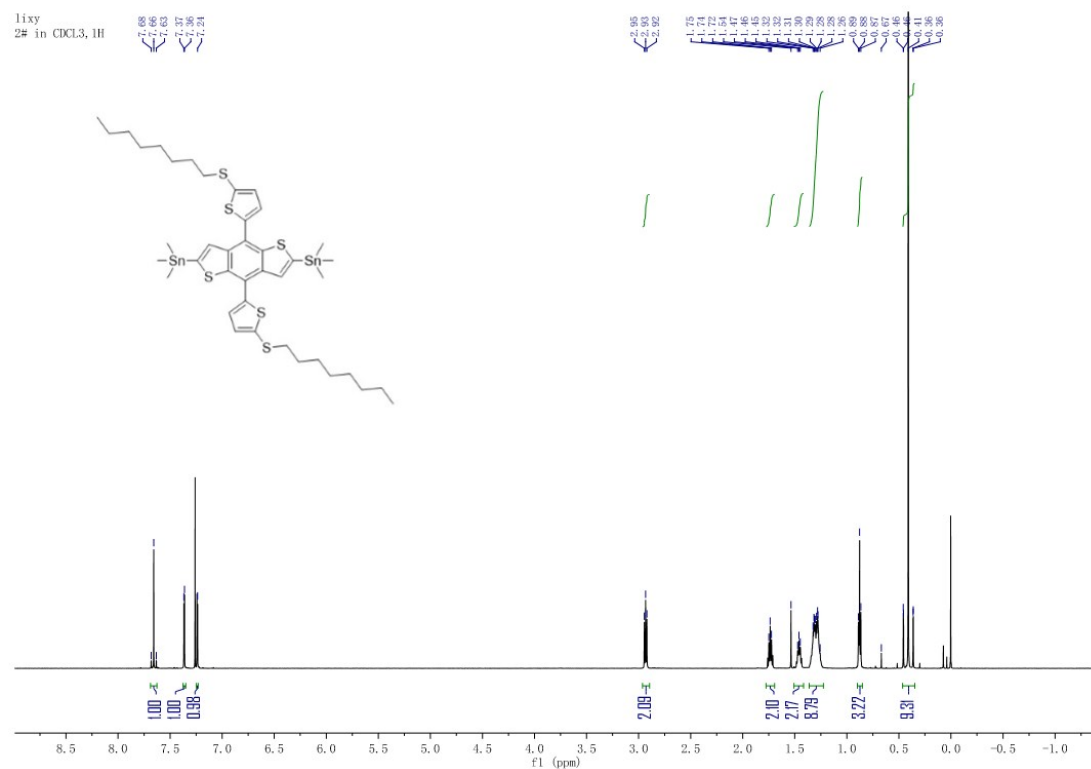


Figure S10 ¹H-NMR of BDT-TSC8-2Sn

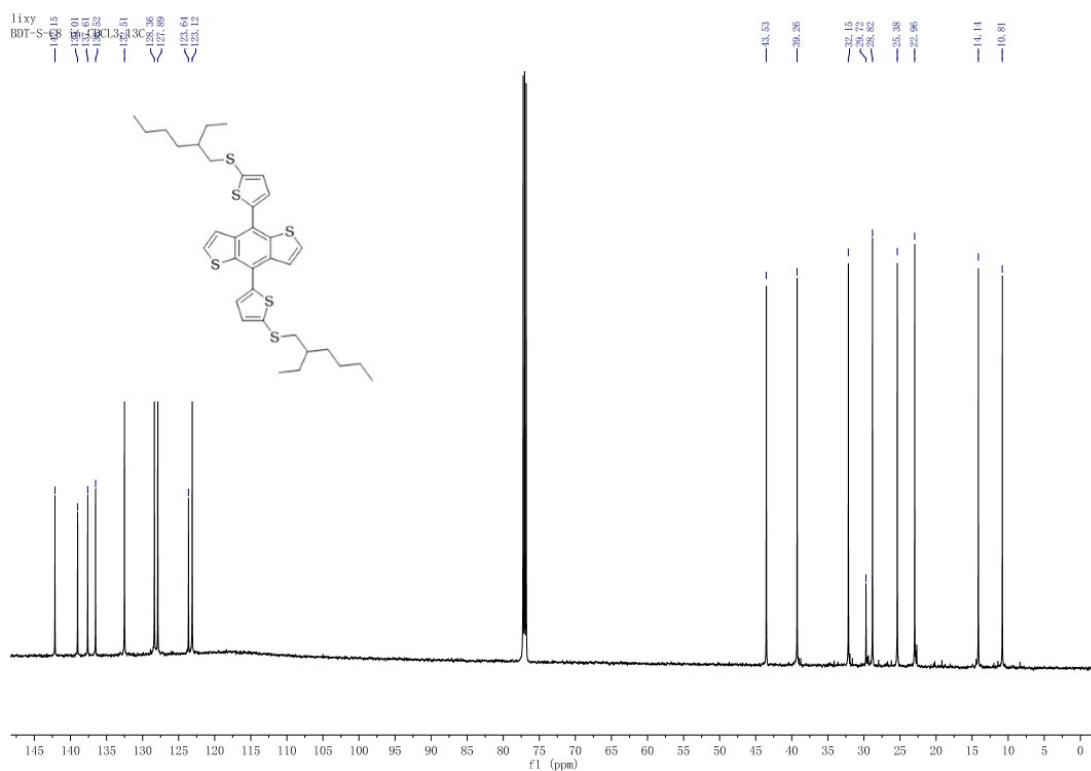


Figure S11 ^{13}C -NMR of BDT-TSEH

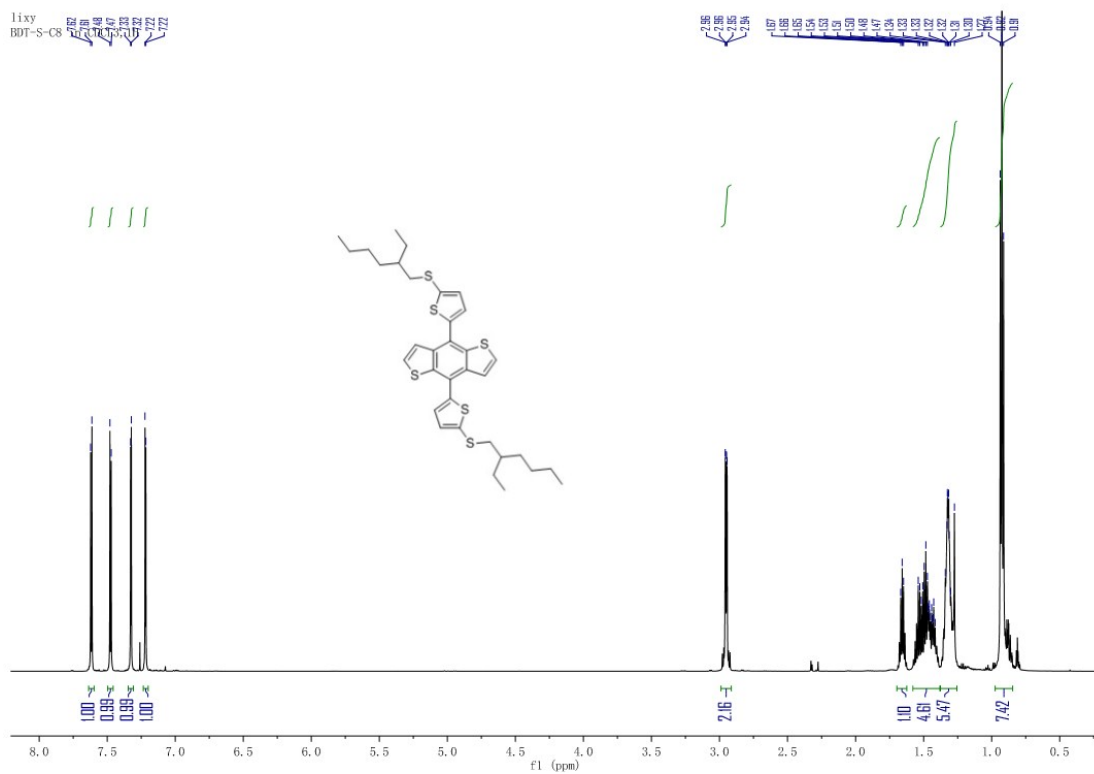


Figure S12 ^1H -NMR of BDT-TSEH

lixy
PBDT-TSC8-Qx in CDCl₃, 1H

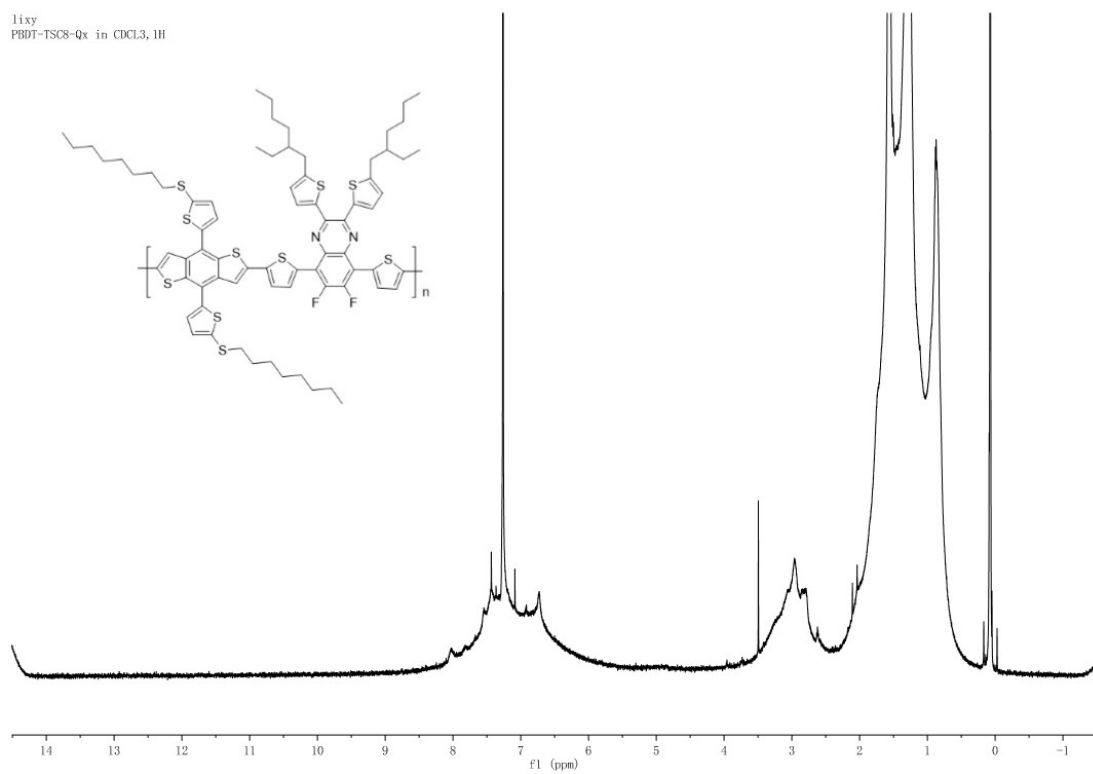


Figure S15 ¹H-NMR of PBDT-DFQ_x-TTSC8

lixy
PBDT-TSEH-Qx in CDCl₃, 1H

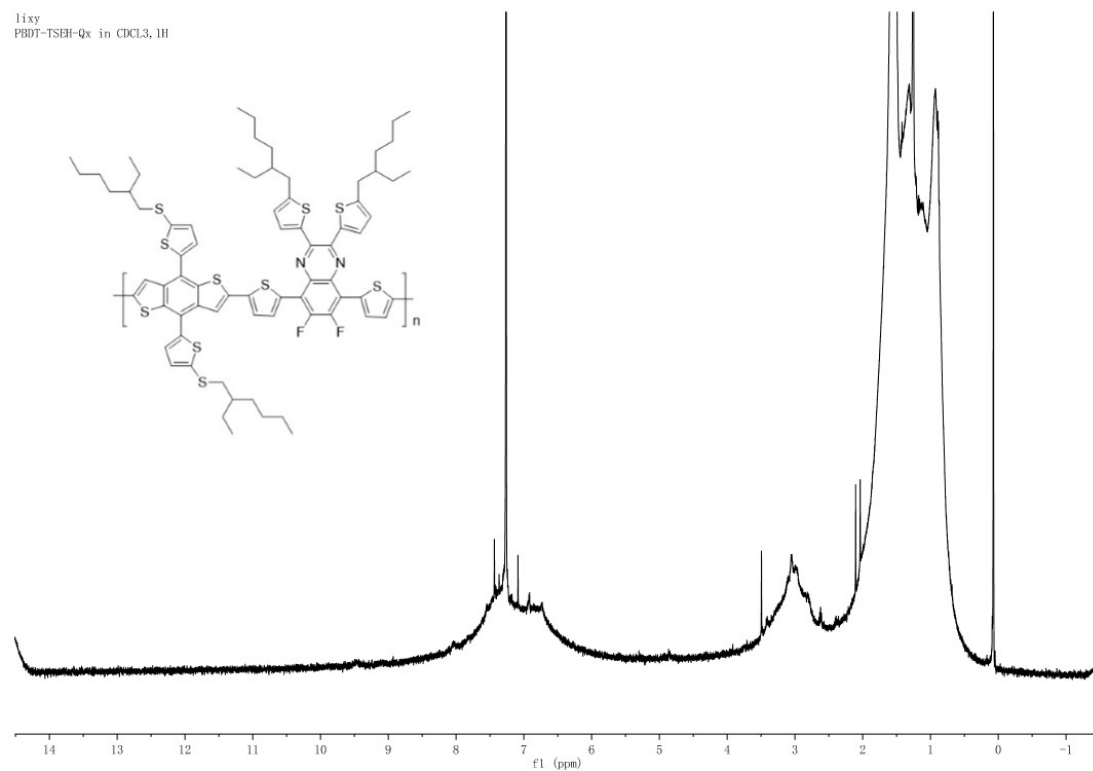


Figure S16 ¹H-NMR of PBDT-DFQ_x-TTSEH